

1 **Supplementary material of :**

2 **“What can we learn from observed temperature and salinity isopycnal anomalies at eddy generation sites?**

3 **Application in the Tropical Atlantic Ocean”**

4

5 Aguedjou H. M. A.^{1,2}, A. Chaigneau^{1,3,2}, I. Dadou¹, Y. Morel¹, C. Pegliasco⁴, C. Y. Da-Allada^{3,5}, E. Baloïtcha²

6

7

8 ¹LEGOS, University of Toulouse, CNRS, IRD, CNES, UT3, Toulouse, France

9 ²CIPMA/UAC, Cotonou, Benin

10 ³IRHOB, Cotonou, Benin

11 ⁴CLS, Ramonville Saint-Agne

12 ⁵UNSTB, Abomey, Benin

13

14

15

16

17

18

19

20

21

22

23

24

25

26

27

28

29

30

31

32

33

34

35

36

37 1. Argo Data quality control and interpolation

38 A total of 144033 vertical temperature and salinity profiles acquired by Argo floats in the TAO and
39 flagged as goof (Argo quality flag 1) were quality controlled following [Chaigneau et al. \(2011\)](#) and [Pegliasco et](#)
40 [al. \(2015\)](#). First, we retained profiles for which: i) the shallowest data is not deeper than 15 m depth and the
41 deepest acquisition is below 950 m depth, ii) at least 30 data are available between the surface and 950 m depth
42 and iii) the depth difference between two consecutive data does not exceed a given threshold (25 m for the 0–
43 150 m layer, 50 m for the 150–300 m layer, 75 m for the 300–500 m layer and 100 m below 500 m depth).
44 Second, each profile was visually inspected and was systematically discarded if it presented a suspicious Θ/S
45 profile. The remaining 114440 profiles, representing ~80% of the original database, were then linearly
46 interpolated every 5 m from the surface to 300m, and every 10m from 300m of depth to the deepest available
47 level. We here assumed that the shallowest values (within 0-15 m depth) were representative of the surface
48 values.

49 2. Weighted arithmetic means.

50 Isopycnal Θ'/S' were computed for each profile by removing a local climatological profile
51 representative of the large-scale background, also computed on density-coordinates. These local climatological
52 profiles (\bar{P}) were obtained by weighted arithmetic means of all the available profiles (P_i) acquired outside
53 eddies, within a radius of 200 km and separated by less than ± 30 days (independently of the year) from the date
54 of the considered profile.

55 Weighted arithmetic mean profiles (\bar{P}) were computed by equation E1:

$$56 \quad \bar{P} = \frac{1}{\sum \Omega_i(r_i, t_i)} \sum \Omega_i(r_i, t_i) \cdot P_i(\rho) \quad (\text{E1})$$

57 where Ω_i are the weights, assigned to each profile, which depend on the distance (r_i) and time (t_i) of the
58 profile P_i (outside eddies) from the considered profile (located inside the eddy):

$$59 \quad \Omega_i(r_i, t_i) = e^{-\frac{1}{2} \left[\left(\frac{r_i}{\Delta R} \right)^2 + \left(\frac{t_i}{\Delta t} \right)^2 \right]} \quad (\text{E2})$$

60 where $\Delta R = 100$ km and $\Delta t = 15$ days are the typical length and time scales. The choice of ΔR and Δt does not
61 significantly alters \bar{P} and the results presented in the study.

62 3. Temperature anomaly threshold

63 In order to determine whether Θ'/S' obtained within eddies are significant or not, a climatology of
64 monthly isopycnal Θ' thresholds was computed on a $1^\circ \times 1^\circ$ longitude/latitude grid within surface and subsurface
65 layers. The surface layer extends from the base of the mixed layer to the base of the seasonal pycnocline and the
66 subsurface layer extends from the base of the pycnocline to the deepest isopycnal level (Fig. S1). As in [de Boyer](#)
67 [Montégut et al. \(2004\)](#), the mixed layer depth was defined as the depth where the density increased by 0.03 kg.m

68 $^{-3}$ from its value at 10 m depth. The reference depth was chosen at 10 m in order to avoid the strong diurnal cycle
 69 that occurs in the first few meters of the ocean (de Boyer Montégut et al. 2004). The base of the pycnocline was
 70 determined as the depth of fluid layer possessing one half of the squared buoyancy frequency (see [Cheng and](#)
 71 [Hsu, 2014](#)). The square buoyancy is defined as :

$$72 \quad N^2 = \frac{-g}{\rho} \frac{d\rho}{dz} \quad (E_3)$$

73 where g , ρ and z , are gravity, density, and depth, respectively.;

74 In both the surface and subsurface layers (Fig. S₁), the monthly climatological Θ' thresholds was computed at
 75 each grid point as follows: first, we selected all the profiles within 200 km around the grid point, that surfaced
 76 outside eddies during the corresponding month (regardless of the year). Second, we computed for each profile,
 77 the square root of the quadratic mean of Θ' integrated over the layer thickness using equation E₄.

$$78 \quad M_1 = \sqrt{\frac{1}{\sum h(\rho_i)} \cdot \sum h(\rho_i) \cdot (\theta'(\rho_i))^2} \quad (E_4)$$

79 where $h(\rho_i)$ and $\Theta'(\rho_i)$ are the thickness and the temperature anomaly of the isopycnal layer ρ_i . Third, we
 80 retained the 80th percentile of M1 values as the monthly Θ' threshold at the considered grid-point. This percentile
 81 was carefully chosen after a sensitivity study and is considered as significantly different from noise. For
 82 accuracy reasons, at least 30 monthly profiles are required around the grid-point to compute the threshold.
 83 Figures S₂ and S₃ show the monthly Θ' threshold distributions for the surface and subsurface layers. Note the
 84 relatively high Θ' threshold within the frontal zone throughout the year in both layers. No strong seasonality was
 85 observed, except a slight increase of the Θ' threshold value in February in the surface layer (Fig. S1).

86 Isopycnal Θ' observed in an eddy is considered as significant if its M1 values in surface and/or
 87 subsurface are higher than the corresponding thresholds shown in Fig. S2-S3. In contrast if the M1 values in the
 88 eddy are lower than the corresponding thresholds in both the surface and subsurface layers, the eddy anomalies
 89 are classified as non-significant. When an anomaly is significant in a given layer, its sign is given by that of the
 90 mean Θ' computed over the layer, as follow:

$$91 \quad M_2 = \frac{1}{\sum h(\rho_i)} \cdot \sum h(\rho_i) \cdot \theta'(\rho_i) \quad (E_5)$$

92 where $h(\rho_i)$ and $\Theta'(\rho_i)$ are the same as for the E₄. A similar formula was used by [Itoh and Yasuda \(2010\)](#) to
 93 identify warm and cold eddies in the northwestern Pacific ocean.

94

95

96

97

98

99

100

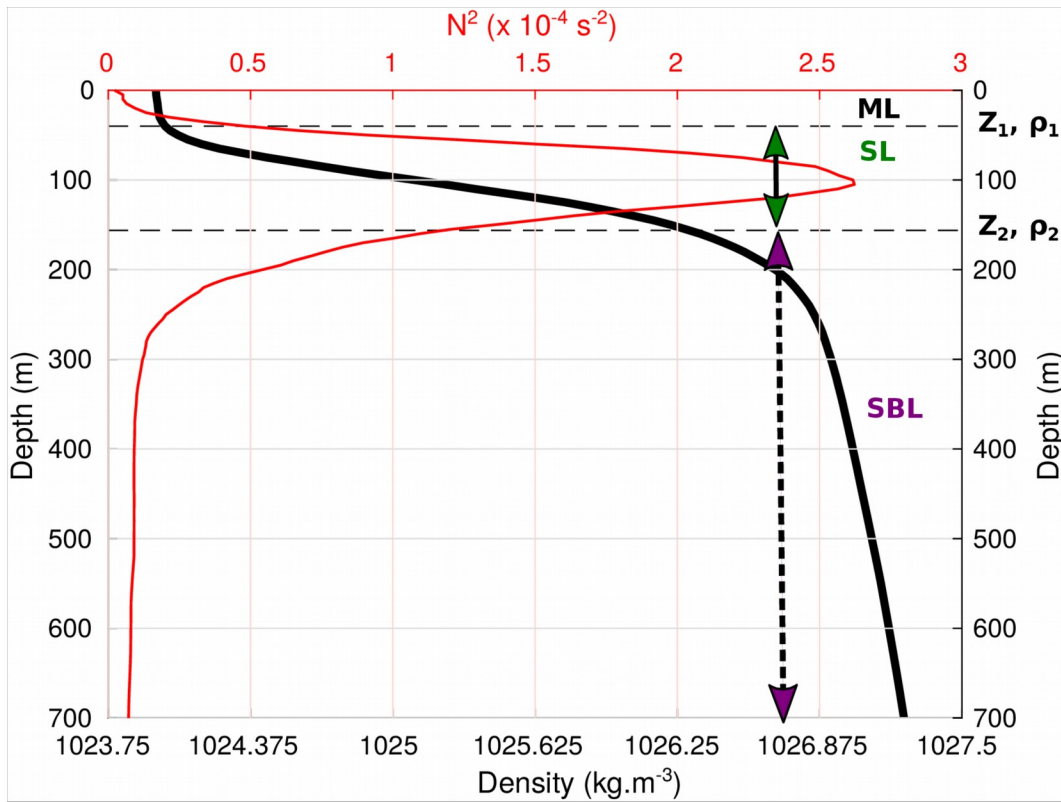
101

102

103

104

105

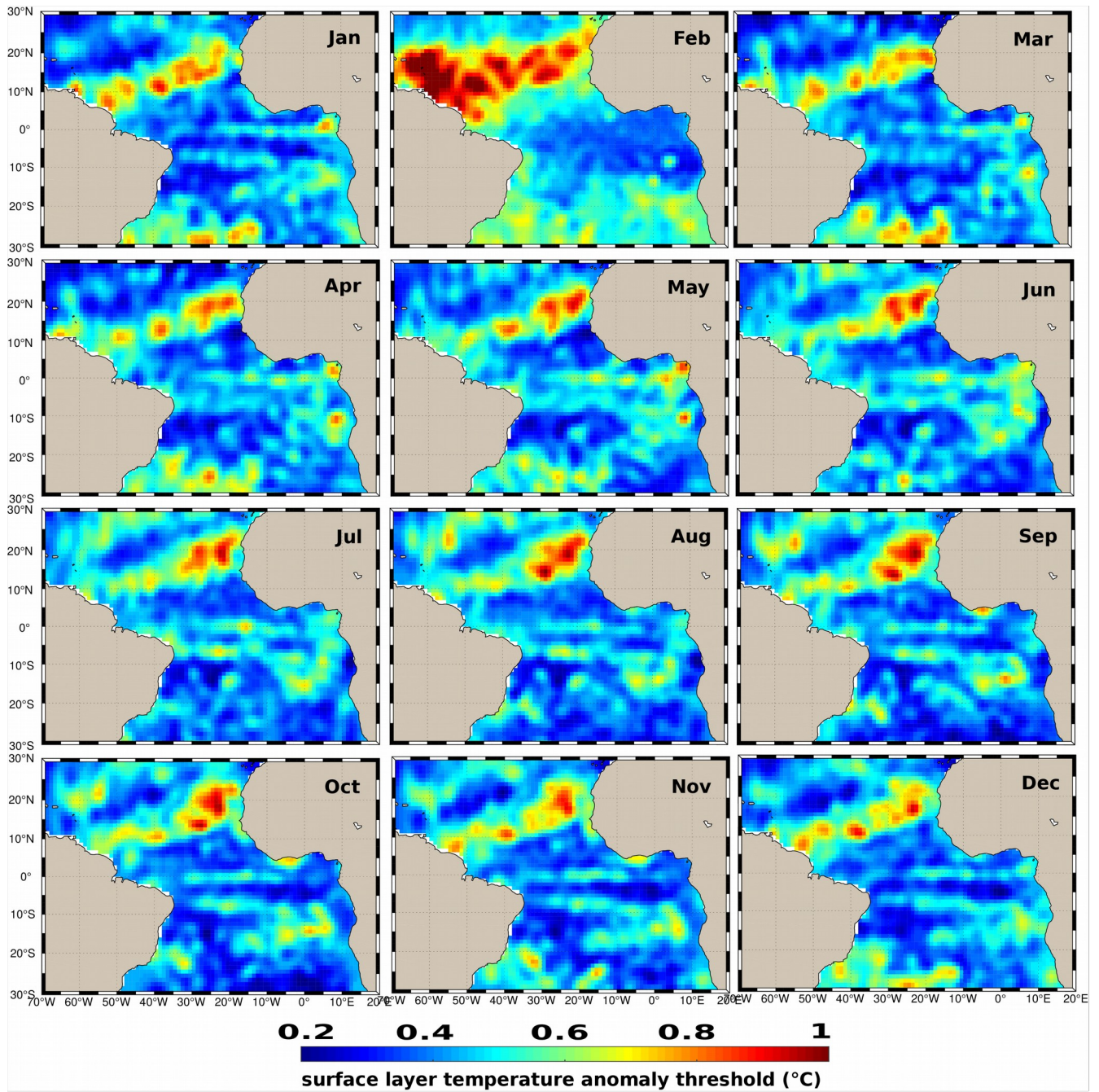


106

107

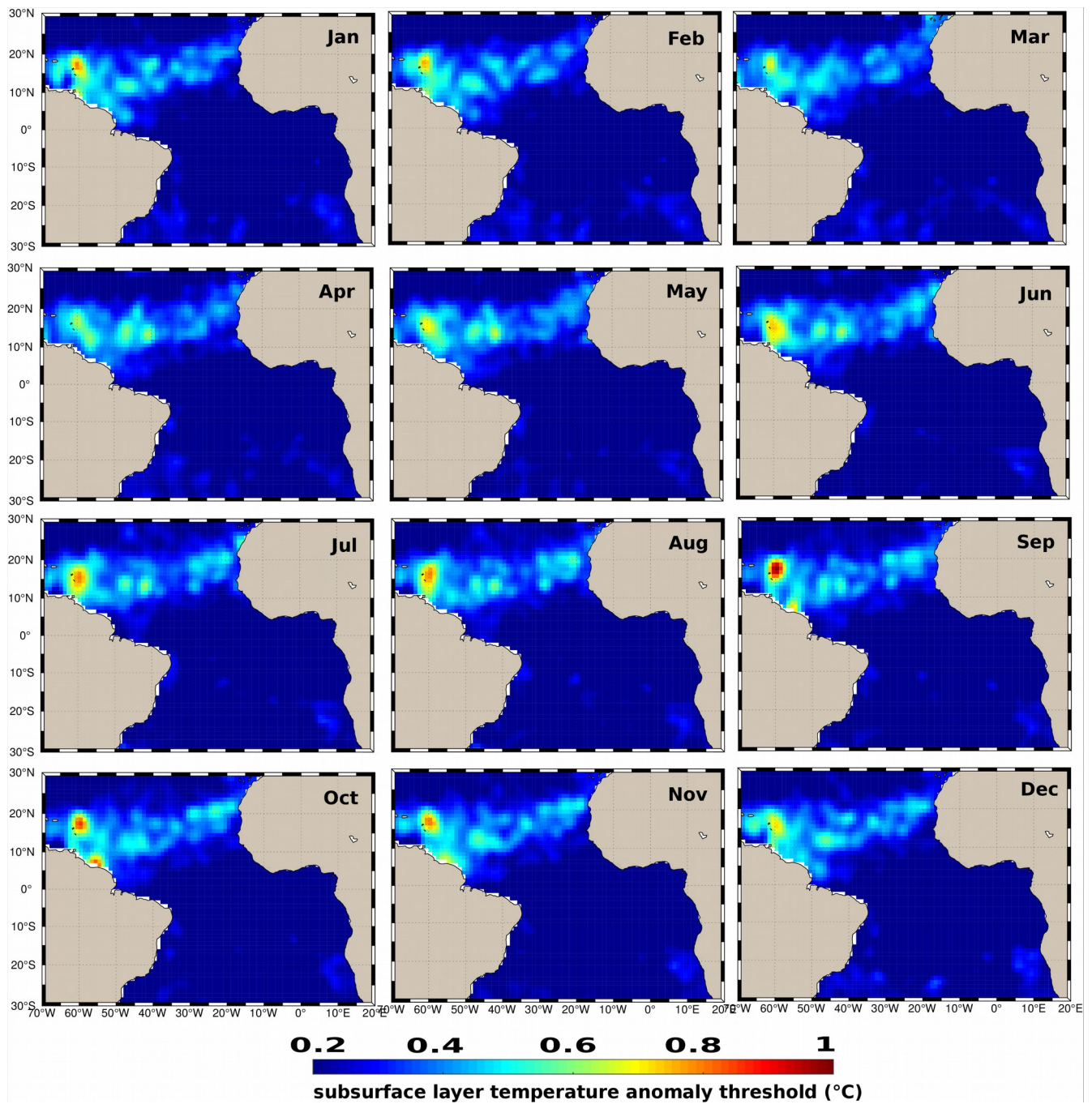
108 **Figure S₁**: Mean density (black curve) and square buoyancy frequency (red curve) profiles at a given grid point
109 showing the mixed (ML), surface (SL) and subsurface (SBL) layers. (Z₁, ρ₁) and (Z₂, ρ₂) are the mixed layer and
110 the base of the pycnocline depths and densities.

111



113 **Figure S2:** Monthly mean of the temperature anomaly threshold within the surface layer.

114



115 **Figure S₃**: Monthly mean of the temperature anomaly threshold within the subsurface layer.

116

117

118

119

120 **References**

- 121 Chaigneau, A., Le Texier A., Eldin G., Grados C., and Pizarro O. (2011), Vertical structure of mesoscale eddies
122 in the eastern South Pacific Ocean: A composite analysis from altimetry and Argo profiling floats,
123 *Journal of Geophysical Research*, 116(C11), doi:10.1029/2011jc007134.
- 124 Cheng, M.-H., and J. R.-C. Hsu (2014), Effects of varying pycnocline thickness on interfacial wave generation
125 and propagation, *Ocean Engineering*, 88, 34–45, doi:10.1016/j.oceaneng.2014.05.018.
- 126 de Boyer Montégut, C., G. Madec, A. S. Fischer, A. Lazar, and D. Iudicone (2004), Mixed layer depth over the
127 global ocean: An examination of profile data and a profile-based climatology, *J. Geophys. Res.*, 109,
128 C12003, doi:10.1029/2004JC002378.
- 129 Itoh, S., and I. Yasuda (2010), Water Mass Structure of Warm and Cold Anticyclonic Eddies in the Western
130 Boundary Region of the Subarctic North Pacific, *Journal of Physical Oceanography*, 40(12), 2624–2642,
131 doi:10.1175/2010jpo4475.1.
- 132 Pegliasco, C., Chaigneau, A., & Morrow, R. (2015), Main eddy vertical structures observed in the four major
133 Eastern boundary upwelling systems: *J. Geophys. Res. Oceans*, 120, 6008- 6033.